9th Asia-Pacific Conference on Wind Engineering
Auckland, New Zealand
3-7 December 2017

LES of wind effects on super-tall buildings with cross-validation by wind tunnel and field measurement

B.W. YAN[1], K.K. Liu[1], Q. YAN[1], Y.Z. Tao[1,2] and Q.S. Li[3]

[1] Key Laboratory of New Technology for Construction of Cities in Mountain Area (Ministry of Education), School of Civil Engineering, Chongqing University, Chongqing, China

[2] School of Civil Engineering, Chongqing University of Science and Technology, Chongqing, China

[3] Department of Architecture and Civil Engineering, City University of Hong Kong, Tat Chee Avenue, Kowloon, Hong Kong

Abstract

This paper presents a cross-validation study of Large-eddy simulation (LES) of wind effects on a super-tall building with surrounding buildings by wind tunnel testing and full-scale measurement. To validate the numerical simulations, the wind tunnel experiments including synchronous multi-pressure and high-frequency force balance model tests are conducted in a boundary layer wind tunnel laboratory. The numerical predictions are then compared with the experimental results, and the comparison demonstrates that the LES can provide comparable predictions of wind effects on the super-tall building. Furthermore, the cross-validation of the predicted displacement responses by the LES against the wind tunnel and full-scale measurements is presented and the agreement among them is reasonably good.

Introduction

Due to the increasing applications of CFD in various problems recently in the current wind engineering study and practical design of buildings, wind load evaluations by CFD has inspired a high demand among designers in the structural design of buildings and structures. And it has been noticed by the wind engineering community that CFD has become a useful tool for engineering practices rather than previously limited use in research or education. At the same time, concerns about the applications of CFD in practical wind engineering problems without careful and professional inspections are widely raised by wind engineering/CFD experts. Since non-experts can easily access the CFD tools, it is not just possible but probable that there exists potentially poor quality and unexpected error levels in CFD simulations performed by structural designers with insufficient knowledge of wind engineering and bluff body aerodynamics. Therefore, it is of great urgency and significance to release the guidelines and perform the benchmark studies for wind load estimations.

The increasing emergences and significant improvements of various CFD software programs encourage the widespread use of CFD techniques at practical design stages. And this also necessitates the demands of best practice guidelines (BPG) to diminish the misuse of CFD commercial software and assure the quality of CFD results to a certain level. To date, some guidelines on industrial computational wind engineering (CWE) applications have been released for validation and verification of CFD techniques. In Europe, Franke et al. led a Cooperation Group of Scientific and Technical Research (COST) to compile a set of guidelines from a comprehensive literature review. And the COST guidelines provide specific and systematic recommendations on the use of CFD in wind engineering, which mainly focus on steady RANS simulations and include limited information pertinent to URANS, LES, and hybrid URANS/LES. In Japan, two AIJ guidelines for CFD applications in structural wind engineering and environmental wind engineering fields have been published by two AIJ working groups. And the necessity of inflow turbulence generation methods for LES has been emphasized for the prediction of peak-type quantities. In addition, a bunch of choices and parameters for RANS simulations of environmental wind engineering have been tested and provided in the AIJ guidelines for the industrial CFD users. The existing and comprehensive guidelines have witnessed the significant progress of CFD for practice engineering in CWE and presented a detailed and interim summary of the available CFD technologies and methods as well as the engineering application procedures. Eventually, they will lay the foundation for the authoritative and abundant codes and standards of CFD In wind engineering, which can significantly promote the engineering applications of CFD.

On the other hand, to significantly increase uptake and engagement of CFD in the evaluation of wind effects on buildings and structures, it is of great necessity to focus on the validation and verification of CFD techniques through cross-comparison with the wind tunnel experiments and full-scale measurements. To date, several validation studies have been performed against the wind tunnel tests using LES in the context of surface pressure distributions, wind forces and wind-induced responses of tall buildings. Recently, the focus for the validation of LES of wind effects on buildings and structures in CWE has shifted to the scenario of a tall building with surrounding buildings rather than on an isolated building, since almost all tall buildings completed, being constructed and at the design stage are located in a high-density city centre. As a consequence, it is of great necessity to perform the comprehensive validation studies of LES against wind tunnel tests and full-scale measurements for evaluation of fluctuating wind loads and structural responses of a surrounded tall building.

The current study focuses on the cross-validation of LES evaluations of wind effects on a super-tall building with surrounding buildings by wind tunnel tests and field measurements. In section 2 a brief introduction of wind tunnel tests, field measurements and LES is presented. The comparison between the LES results and the wind tunnel tests and field measurements is presented in section 3. Finally, the conclusions of this study are summarized in Section 4.

Field measurements, wind tunnel and LES

Wind tunnel tests

The wind tunnel test was conducted in the Boundary Layer Wind Tunnel Laboratory (BLWTL) at the City University of Hong Kong (CityU) as shown in Fig. 1. The dimensions of the test section are 4.0m in width and 2.0m in height, and the layout of the test models which were replicated at a scale of 1:400. The test models consist of two parts: a detailed model of the super-tall building as indicated in Fig. 1, and the proximity models of buildings surrounding the super-tall building within a radius of 600m (in full scale). Using ground roughness, spires and fences in the wind tunnel, profiles of longitudinal mean wind speed and turbulence intensity were generated. Referring to a suburban terrain (Category III) suggested by Architectural Institute of Japan Recommendations for Loads on Buildings (2004), the profile of mean wind speed was fitted by a power law exponent of 0.20, and that of turbulence intensity was fitted by a power law exponent of -0.25. The selection of the wind profiles corresponding to a suburban terrain (Category III) was a compromise between the facts, due to the fact that the north of the super-tall building is an open water terrain (Category I) while the south of the building is a densely built-up city terrain (Category V). In the wind tunnel test, the longitudinal mean wind speed and turbulence intensity at the roof height of the building model were 8.47 m/s and 9.5%, respectively. Thus, Reynolds number of simulated wind flows is approximately 6×104, which is adequately high for a building having sharp corners in its cross-sections. On the other hand, according to the Code of Practice on Wind Effects in Hong Kong (2004), the full-scale wind speed having a return period of 50 years at the building roof height (420m) is 58m/s, which results in a velocity scale of approximately 1:7 for the wind tunnel test. By rotating the turntable beneath the test models, total 24 different approach wind directions at the increment of 15° were considered in the wind tunnel test.

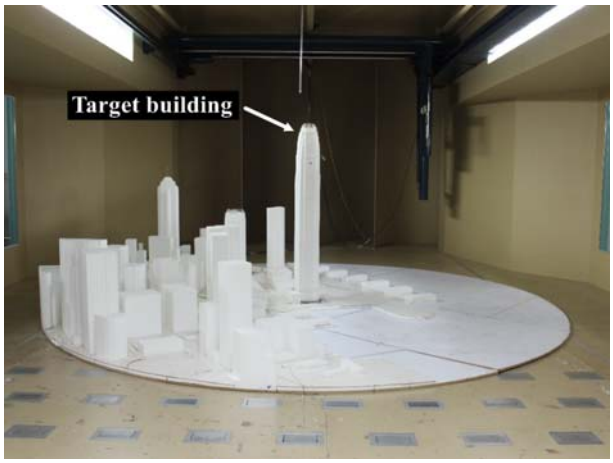

Fig. 1 Photo of the wind tunnel test section and test model layout

Field measurements

This study employs the field measurements by a SHM (Structural Health Monitoring) system installed in a 420 m high super-tall building. As indicated in Fig. 1(a) and Fig. 1(b), the monitored building, denoted by BLD (22°17'7", 114°09'33"), is located on the north coast of Hong Kong Island (peak height is 552m AMSL), with a large number of tall buildings with height over 150m located adjacently to its east, south and west. The distance between the building and the foot of Hong Kong Island is less than 1 km. Separated by Victoria Harbor with a width about 2km, Kowloon Peninsula lies in the north of Hong Kong Island. From Fig. 1(b), SSP and KP stations in Kowloon Peninsula are located in the north-northeast of the super-tall building with a distance of 4.8 km and 3.3 km, respectively.

As shown in Fig. 2(a), the monitored tall building's exterior shape is of a convex-square whose sectional width gradually tapered from 57m to 39m with height. To enhance the lateral resistance to wind loads, the building adopts a hybrid structural system which consists of steel beams and outriggers to link the building's reinforced concrete central core to eight exterior composite mega-columns. The approaching wind speed and direction atop the super-tall building and its structural responses were measured by a Gill WindMaster Pro 3-Axis ultrasonic anemometer and a pair of accelerometers, respectively. As shown in Fig. 2, the ultrasonic anemometer was installed about 14m above the roof of the building, or 419.3m AMSL, while a pair of accelerometers were placed at the centre of the building's top floor at a height of 398.9m AMSL which are orthogonally placed in directions X and Y. By convention, 0° and 90° directions of horizontal wind measured by the anemometer represent the north and east, respectively. It is worth noting that there is an angle difference of 32° between direction Y and the north. Both the anemometer and the accelerometers collected the field data at a sampling frequency of 20Hz. These data were recorded synchronously by a data acquisition unit, and can be displayed continuously in real-time through the control panel of the SHM system shown in Fig. 2(d).

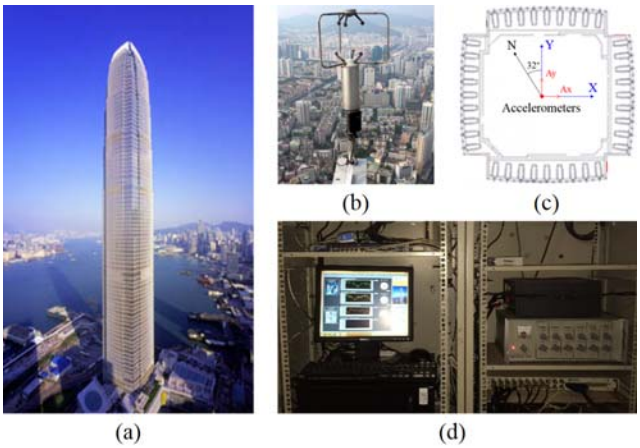

Fig. 2. The super-tall building and its SHM system: (a) building exterior; (b) ultrasonic anemometer; (c) locations of the accelerometers and orthogonal directions X and Y; (d) control panel of the SHM system

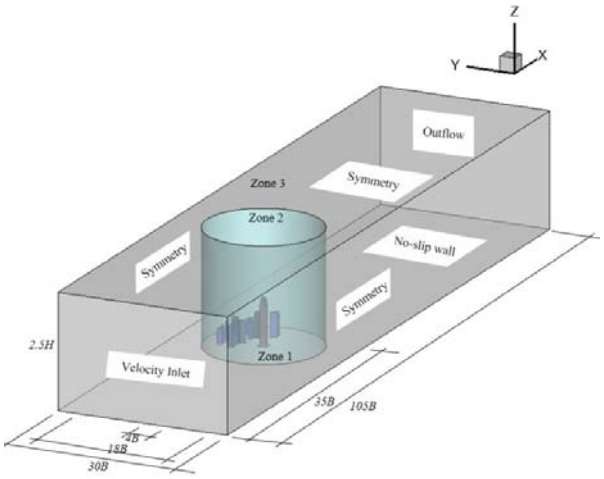

Fig. 3 Computational domain and boundary conditions

LES

The geometric model for LES was established in the same sale as that in the experiments. The dimensions of the computational

domain were 15m (x) × 4m (y) × 2.5m (z). The blockage ratio determined by the maximum projection area in the streamwise direction is less than 3%, which is generally accepted in CWE.

The difficulty encountered in mesh generations is due to the complex building shapes, which makes it fairly challenging to discretise the whole computational domain with structured meshes (hexahedral elements). Hence, the multi-block technique was utilized to split the whole domain into three blocks as depicted in Fig. 3. The super-tall building model was nested in "Zone 1", which was filled with unstructured meshes (tetrahedral and prismatic elements) to accommodate the complex geometry of the building as shown in Fig. 4. Similarly, the unstructured meshes were generated in "Zone 2" to represent the surrounding buildings. And structured meshes were adopted in the subdomains of "Zone 3". The advantages of the combination of the nesting grid and the multi-block technique are: (1) reducing the total grid number by hybrid use of coarser hexahedral elements in the external region and finer tetrahedral and prismatic elements in the inner region; (2) flexibility, efficiency and accuracy in the mesh generation for complex building shapes in urban areas; (3) easing the tedious labor work in grid generations, particularly when changing the approach wind direction, which can be accomplished by rotating the subdomain "Zone 3" and its connecting meshes. The minimum and maximum grid lengths on the building surfaces are 5×10^{-4} m and 2.5×10^{-3} m, respectively. In the subdomains "Zone 1" and "Zone 2", the grid stretching ratio in the horizontal direction was kept to be less than 1.03, while that in "Zone 3" is 1.05. The relatively small stretch ratios reduce the differences of cut-off wave number between the neighbouring grids. The total grid number of the super-tall building model with surrounding buildings was approximately 5.4×10^{6}.

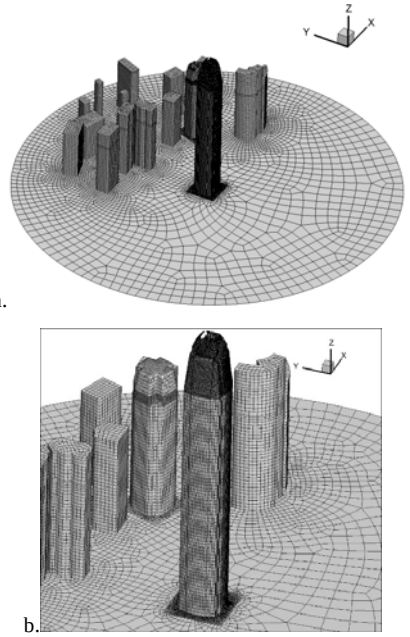

a.

b.

Fig. 4 Mesh arrangement

Inflow turbulence generation

Inflow boundary condition (IBC) is generated using both the Discrete Random Flow Generator (DRFG) and Consistent Discrete Random Flow Generator (CDRFG) techniques [1]. The key parameters of IBC are summarized in Table 1.

Parameter	Definition	Value(s)
Exposure	Open terrain	U_{avref}=8.47m/s
Mean velocity U_{av}	$U_{av}=U_{avref}\left(\frac{z}{z_{ref}}\right)^{\alpha}$	z_{ref}=1.0m α=0.2
Turbulent intensity I	$I_j=I_{refj}\left(\frac{z}{z_{ref}}\right)^{-\beta_j}$	I_{refj}=0.095; β_j=0.25
Length scale	$L_j=L_{refj}\left(\frac{z}{z_{ref}}\right)^{\varepsilon_j}$	L_{refj}=0.64 and ε_j=0.12
Coherency function	$\mathrm{Coh}(f_m)=\exp\left(\frac{C_j f_m dx_j}{U_{av}}\right)$	C_f is coherency decay constant
Frequency parameter		$f_{m\ \min}$=1.0Hz; M=100 $f_{m\ \max}$=100Hz, N=50; Δ_f=1.0Hz

Table 1 Parameters used for generating velocity field

Boundary conditions

In the present numerical simulations, in order to reproduce the wall-induced turbulence, the near-wall treatment proposed by Werner and Wengle was applied on the building surfaces and ground. In this method, the wall shear stresses were estimated by analytical integration of the power-law near-wall velocity distribution.

The periodic boundary conditions are used in the spanwise direction and a symmetry condition ($\frac{\partial u}{\partial z}=\frac{\partial v}{\partial z}=0$ and w=0) is adopted at the top boundary. The convective boundary condition was set at the outlet for all flow variables normal to the outflow boundary conditions with an overall mass balance correction.

Turbulence model

The dynamic Smagorinsky-Lily model by Germano et al. was adopted in this study as the default SGS turbulence model. The model constant C_S was determined by the dynamic procedure, which varies in time and space between zero and 0.23, while non-negative value of the constant is taken to avoid numerical instability (Ansys/Fluent, 2013).

Numerical algorithms

In this study, all the discretized equations were solved in a segregated manner with the pressure implicit with splitting of operators (PISO) algorithm. Second-order discretization schemes were adopted for time and spatial discretization. Bounded central differencing (BCD) was used for momentum discretization. The time derivative was discretized using the second-order backward differences and the spatial discretization was treated implicitly. The least squares cell based method was used for numerical approximation of gradients.

The LES was performed with the general-purpose commercial code ANSYS /Fluent 15.0. And all the results were obtained from the parallel calculations with 64 CPUs on the High Performance Cluster (HPC) at Chongqing University. Since both the DSRFG and CDSRFG methods possess the merit of efficient implementation in parallel version, it is effectively embedded via paralleled User Define Function (UDF) in the Ansys/Fluent code. All the results from the LES were sampled after an initialization period of 5000 time steps or approximately 6.7 flow-through times ($T_{ft}=L_x/U_H$, where L_x was the length of the computational domain in the longitudinal direction (x) and U_H was the reference mean wind velocity). The total time steps were 20,000, equivalent to almost $30T_{ft}$, which was sufficiently long to reach the statistical convergence for LES.

Results and discussions

Velocity field

The probable cause for errors or discrepancies in some previous CWE applications was an improper inflow boundary conditions imposed at the inlet. Therefore, the accurate predictions by LES require the inflow boundary conditions match the mean and turbulent inflow conditions of the realistic wind flows in ABL.

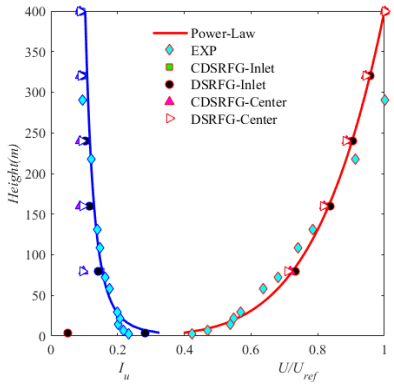

Fig. 5 Profiles of mean wind speed and turbulence intensity

Fig. 5 shows the mean wind speed and turbulence intensity profiles numerically simulated by two inflow turbulence generation methods compared with the experimental inflow conditions. The wind velocity data from the numerical simulations are sampled at the building position downstream from the inlet plane to estimate the influences of the grid resolution on the grid-filtered velocity components. It can be found in Fig. 5 that the numerically simulated mean speed profiles by the different methods agree well with the target profiles. Meanwhile, the profiles of longitudinal turbulence intensity slightly deviated from the target profile in the lower height at the area of concern; although the good agreement is observed at the inlet. This indicates that the synthetic inflow turbulence might decay with the distance away from the inlet plane so that the turbulence level superposed at the inlet cannot be well sustained until the flow reaches the location of the target building. A reasonable explanation for this phenomenon is that because the grid length is used as a filter width in the LES to separate turbulence into large eddies and small eddies, the smaller grid spacing or filter width is, the larger the range of eddy scales is resolved directly by the LES rather than by the SGS model.

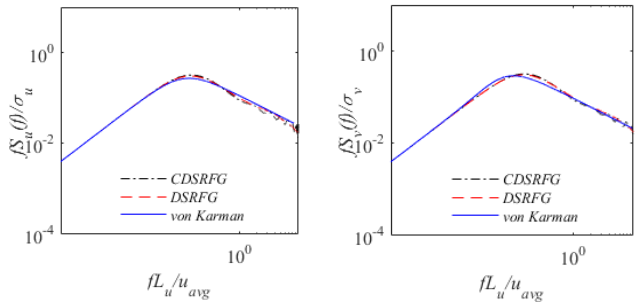

a. Streamwise b. lateral

Fig. 6 Vleocity spectra

Fig. 6 shows the spectral features of synthetic turbulence generated by both the CDSRFG and DSRFG method. The power spectral densities (PSDs) of fluctuating velocity components in all the x-, y- and z-directions follow a slope of -5/3 reasonably well in the inertial sub-range. And both the velocity spectra are in good correspondence with the specified von Karman spectrum model in the streamwise and lateral directions.

Building responses

The full-scale data are scattered against the 10 minutes averaged wind speed atop the building in both x and y directions. The curves from the LES and the wind tunnel testing generally envelope the scattered field measured data and show a similar trend among them.

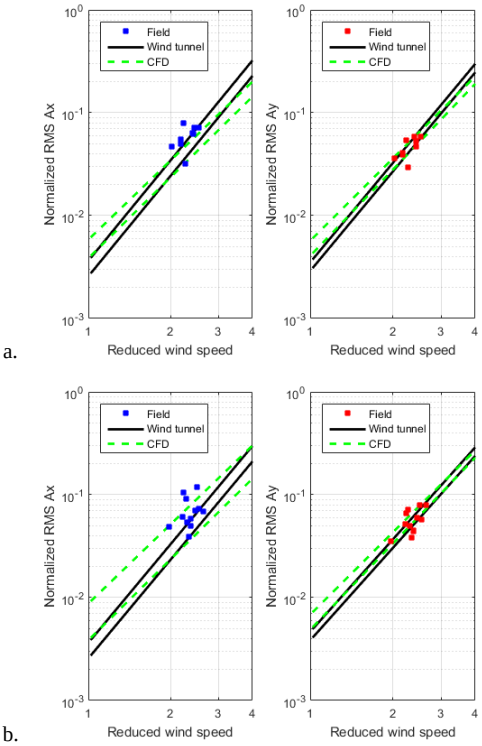

a.

b.

Fig. 7 Comparison of top floor peak (a.) and RMS (b.) accelerations between wind tunnel tests, field measurments and LES

Conclusions

(1) The DSRFG method was proven to be able to generate the anisotropy of the ABL flow with the prescribed velocity spectra and turbulence properties including turbulence intensity and turbulence integral length scale. Inadequate grid resolution between the inlet and the area of interest resulted in lower turbulence levels before the flow reached the concerned buildings' locations. Therefore, it is necessary and critical to perform the grid-sensitivity study in an empty computational domain to determine the proper mesh scheme.

(2) The wind loadings on the super-tall building predicted by the LES were comparable to the wind tunnel measurements, including the mean and RMS pressure coefficients, local wind force spectra, base force and torsional moment spectra as well as the statistics of fluctuating pressures and base forces.

(3) Through the cross-validation of the top displacements of the super-tall building (resonant, background and total displacements), it was found that the predictions by the LES were in reasonable agreement with the full-scale measurements and the wind tunnel experimental results.

In summary, the LES technique and the numerical treatments adopted in the present study offer a promising and effective approach for estimation of wind effects on tall buildings in the urban environment.

Acknowledgments

The work described in this paper was fully supported by the National Natural Science Foundation of China (Grant No.: 51608075), the Fundamental Research Fund for the Central University (Grant No.: 106112016CDJXY200010 and 106112017CDJQJ208849) and Environment and Conservation Fund (ECF) of Hong Kong (Grant No.: 9211097).

References

[1] Aboshosha, H., Elshaer, A., Bitsuamlak, G.T., & Damatty, A.E., *J. Wind Eng. Ind. Aerodyn.*, 142, 2015, 198-216.